GREEN FLUORESCENT PROTEIN AS A BIOSENSOR FOR TOXIC COMPOUNDS

Renato J. Aguilera*, Jessica Montoya*, Todd P. Primm,
Armando Varela-Ramirez***

1.1 ABSTRACT

In this brief review, we present recent results in the development of fluorescence-based assays for the detection of compounds with cytotoxic, anticancer and anti-microbial properties. As other reviews have explored various aspects related to these topics, this review will focus on the use of the Green Fluorescent Protein (GFP) for the detection of potentially toxic and/or therapeutic compounds.   Since high-throughput screening of chemical compounds can be both expensive and laborious, development of low cost and efficient cell-based assays to determine biological activity should greatly enhance the early screening process. In our recent studies, we have developed a couple of GFP-based assays for the rapid screening of compounds with cytotoxic and bacteriocidal properties. As will be described in more detail in subsequent sections, a new 96-well assay has recently been developed that allows for the simultaneous screening of test compounds on gram positive and negative bacteria as well as mammalian (human cancer) cells. Our results demonstrate that both mammalian cells and bacteria can be analyzed in tandem to rapidly determine which compounds are specifically toxic to one of these cell types. The parallel screening of both eukaryotic and prokaryotic cells was found to be feasible, reproducible, and cost effective.

1.2. BRIEF OVERVIEW ON THE PROPERTIES OF GFP

Few methods exist that allow the visualization of living cells as they undergo apoptotic or necrotic modes of death.   Since labeling of cells with dyes is not always efficient and may lead to interference of cellular functions, the preferred method for non-invasive detection is *via* the use of fluorescent markers. A fluorescent marker that has achieved prominence in visualization assays is GFP and its derivatives. These

*Department of Biological Sciences, University of Texas at El Paso, 500 W. University Dr., El Paso, TX 79968-0519. E-mail: raguilera@utep.edu
** Department of Biological Sciences, Sam Houston State University, Hunsville, TX, 77341

proteins have greatly facilitated the *in vivo* and *in situ* visualization of proteins involved in complex cellular functions.

GFP was first detected in the jellyfish, *Aequorea victoria,* in 1961 [1], but the cloning of the GFP gene did not take place until 1992 [2]. Subsequent expression of the GFP protein revealed that it retained its fluorescence properties in non-jellyfish species (for extensive reviews see [3; 4]).   GFP is an exceptional protein since it does not require co-factors or substrates, is stably expressed as a fusion protein, is relatively non-toxic, and can be readily detected by fluorescence microscopy and other fluorometric techniques (see [3; 4]). The wild type GFP protein has two excitation peaks at 395nm and 470nm, and its emission peak is at 509 nm [4].   However, the most unique feature of GFP is the highly fluorescent chromophore composed of Ser-Tyr-Gly residues which are cyclized and oxidized to form the chromophore [3; 4]. Due to these unusual characteristics, this protein has been used to explore complex biochemical and cellular processes in living cells and in whole prokaryotic and eukaryotic organisms (reviewed by [3; 5]). GFP variants have also been created with shifted absorbance and emission spectra and improved folding and expression properties. The creation of blue, cyan, yellow and red GFP variants coupled with new fluorescence imaging techniques has greatly enhanced our ability to perform localization and kinetics studies of GFP-tagged proteins (see [3] for a review of these techniques).   It is important to note that the majority of recent studies make use of an enhanced version of GFP (EGFP) which is not only codon optimized for mammalian expression but also contains point mutations that make it brighter and more stable [3].

1.3. GFP AS A BIOSENSOR

The use of GFP as a biosensor for genotoxic compounds has also been gaining momentum over the past few years [5-8].   A good example of these assays, is the GreenScreen genotoxicity assay that can simultaneously measure both toxicity and genotoxicity in yeast [9-11].   This assay relies on genetically modified yeast carrying a DNA damage-inducible RAD54 promoter upstream of a yeast-enhanced GFP gene that is expressed when DNA repair is induced by genotoxic agents [6; 11]. A reduction in cell proliferation was used to determine toxicity and to test environmentally relevant substances such as metal ions, solvents, and pesticides. Most recently, this assay was modified for environmental monitoring using portable instrumentation [9]. Using a similar strategy, Normal *et al*, generated GFP-reporters based on the inducible DNA damage SOS response of *Escherichia coli* [12].   Although several constructs were tested, the SOS-GFP biosensor was found to be highly sensitive to the detection of carcinogens and genotoxins [12]. Apart from an increase in sensitivity, as compared to other *E. coli* GFP-based models, this system should be readily applicable to high-throughput screening assays.

The use of GFP-expressing mammalian cells for cytotoxic compound screening was first described by Sandman, *et al.*, [13]. In this study, the inducible Tet-On system was utilized to drive the expression of EGFP in HeLa cells to evaluate the cytotoxicity of platinum complexes [13].   Treatment of the inducible HeLa cells with cisplatin and other platinum complexes resulted in a strong correlation between GFP inhibition and cytotoxicity [13].   The observed decrease in GFP expression was mediated by transcriptional downregulation possibly due to platinum-mediated DNA crosslinking [13].   In another study using well-known cytotoxic agents, Steff, *et al*., [14]

demonstrated that GFP-based assays yielded comparable kinetics and sensitivity to more traditional apoptosis assays. After toxicant exposure, a decrease in GFP fluorescence was detected by flow cytometry and fluorescence-based microplate assays [14]. Although the mechanism for the loss of fluorescence was not determined, cytoplasmic GFP-fluorescence was found to decrease during cell death but this decrease in signal was apparently not due to protein degradation [14]. In yet another study, the fluorescence signal of a fusion protein consisting of GFP and the nuclear pore membrane protein POM121 that targets to the nuclear membrane was also found to dissipate after induction of apoptosis in a neuroblastoma cell line [15]. In this study, the loss of GFP-signal was found to correlate with the degree of chromatin condensation and nuclear DNA fragmentation associated with apoptosis [15].

A novel murine bone marrow stromal cell line has also been established for the assessment of p53 (tumor suppressor) protein responses to genotoxic stress [16]. In this study, EGFP was used to assess the transactivation response of p53 to chemical and physical stimuli. As was expected, GFP expression was significantly enhanced upon exposure to p53 inducers and this induction correlated well with p53 protein accumulation making this model system very useful for toxicological studies. Using a similar approach, Quinones and Rainov [17], established a human cell line (HEK293-TP53::EGFP) that expresses a functionally stabilized p53 protein fused to EGFP to monitor p53 protein expression as well as its subcellular localization. In this system, DNA damaging agents caused a significant increase of intracellular p53-EGFP levels, which was dependent on the endogenous p53 status. These GFP-based reporter systems should be very useful for the identification of mutagens and carcinogens that induce p53 expression.

An interesting twist to the aforementioned assays is the use of GFP-tagged cells in cell-mediated cytotoxicity assays. Analysis of cytotoxic T-lymphocyte (CTL) or natural killer (NK) cell activity generally involves the use of radiolabeled target cells and therefore the creation of sensitive non-radioactive assays is highly desirable. A GFP-based "fluorolysis" method was developed that is significantly more sensitive than the standard ^{51}Cr-release assay for CTL activity [18]. In this assay, the well characterized T-cell target cell line P815 was transfected with the GFP gene and used as a target in CTL assays. Using flow cytometry, the percentage of GFP labeled target cells was easily detected allowing for the identification of a smaller number of activated CTLs [18]. A variant of this assay has recently been employed for the detection of NK-mediated cytolysis. In this case, a GFP-transfected Wilms' tumor cell line was established that is highly susceptible to human NK cells [19]. Measurement of GFP release by NK-lyzed tumor cells was found to correlate well with radioisotopic assays and proved to be a convenient alternative for monitoring human activated NK-cell mediated killing activity [19].

## 1.4. GFP-BASED TOXICITY ASSAYS IN MULTICELLULAR ORGANISMS

Apart from the large variety of prokaryotic and eukaryotic cell based assays, recent breakthroughs allow GFP-detection in live multicellular organisms. For example, a chick-embryo metastatic cancer model has recently been described that makes use of Lewis lung carcinoma cells that express GFP [20]. Injection of the GFP-tagged carcinoma cells into 12th day chick embryos resulted in metastases in the brain, heart, and sternum, which was readily visualized by fluorescence after several days. Co-

injection of the marked cells with therapeutic agents resulted in complete inhibition of metastases indicating that this model can be used for screening of anti-cancer/metastatic drugs [20]. Several GFP transgenic animals have also been generated that could potentially be used to screen the effects of toxic compounds *in vivo*. Most recently, transgenic zebrafish [21; 22], medaka [23], and nematode [24] models have been described for the detection of pollutants and other environmental genotoxic compounds. Transgenic mice expressing GFP have been used for a variety of purposes including analysis of tumor angiogenesis [25] and metastasis [26-28]. A good example of targeted expression of GFP is the non-invasive prostate imaging model in live mice [29]. In this model, transgenic mice carrying the human kallikrein 2 promoter coupled to luciferase and GFP genes, *via* a bi-cistronic vector, yielded animals that specifically expressed GFP in the prostate lobes [29]. In addition, several GFP-tagged cancer cells introduced into immunocompromised mice have been developed that have allowed visualization of tumor growth, metastasis and its associated vascularization [27]. These systems offer great advantages as the GFP-tagged tumor cells are readily detected in normal tissues by fluorescence microscopy without extensive sample preparation. Since the process of metastasis is not fully understood and since prevention of tumor-spread is of great importance for cancer therapy, any insights provided by these cancer-models can lead to the discovery of novel therapeutic approaches. In recent years, intravital microscopic methods and whole body imaging techniques have been developed to detect GFP-tagged tumor progression in animals [25; 26; 30-33]. In fact, real time detection of such labeled cells has been used to detect single cells (reviewed by [27]) and used to monitor the metastatic process [34; 35]. These *ex vivo* detection techniques are highly relevant for the screening of novel therapeutic agents and they may allow the detection of tumor cell clearance during drug treatment.

1.5. RECENT GFP-ASSAYS FOR DRUG DISCOVERY

Since high throughput screening of chemical compounds can be both expensive and laborious, development of low cost and efficient cell-based assays to determine biological activity should greatly enhance the early screening stages [36-38]. Several computational methods are currently in use to predict the potential toxicity of novel compounds but it is highly unlikely that these methods will fully replace animal or cell-based assays [39-42].

In our recent studies, we developed two GFP-based assays for the rapid screening of compounds possessing cytotoxic and bacteriocidal properties [43; 44]. In our first attempt to develop a simple cytotoxicity assay, we made use of a human cancer cell line, HeLa-GFP [45] that constitutively expresses a recombinant EGFP gene fused to histone H2B [43]. Expression of the H2B-GFP fusion protein results in nuclei that can be readily detected by fluorescence microscopy [45]. An obvious advantage of using GFP-marked cells to examine cytotoxicity is that the same cells can be analyzed over a prolonged period of time. As can be seen in Fig. 1, the cytotoxic effects of plumbagin (Q1), a known cytotoxic naphthoquinone, was monitored by fluorescent microscopy over a 10 hour period. Prototypical signs of apoptosis were detected by 6 hours of exposure as evidenced by nuclear DNA condensation and membrane blebbing. After 10 hours of exposure, GFP fluorescence decreased significantly, which was most evident when the cells were treated with another cytotoxic naphthoquinone, 3-Phenyl-

| | 0 hrs | 6 hrs | 8 hrs | 10 hrs |
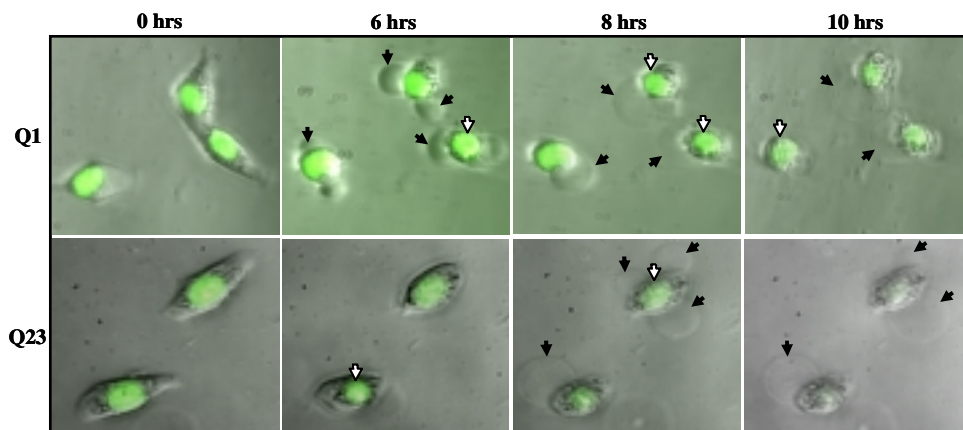
Figure 1. Microscopic analysis of the toxic effects of plumbagin (Q1) and 3-phenyl-1,4-naphthoquinone oxide (Q23).   Using fluorescence microscopy, a group of HeLa-GFP cells was monitored for signs of cell death at two hour intervals over a 10 hour period. Obvious signs of cell-death induction were clearly visible by 6 hours (hrs) of chemical exposure by membrane "blebbing" (see filled arrows) and by an increase in nuclear DNA condensation (open arrows). Note that Q23 (see Fig. 3) is the same compound referred to as NQ11 in our previous analysis [43].

1,4-naphthoquinone oxide; Q23, see Table 1 and ref. [43]). This decrease in GFP-signal is likely due to DNA degradation and the loss of nucleosomal structure. Interestingly, clouds of GFP fluorescence were occasionally detected adjacent to the GFP-depleted nuclei presumably due to release of histones/nucleosomes after inter-nucleosomal DNA cleavage

To eliminate the possibility that the H2B-GFP fusion protein contributed to the cytotoxic effects of the quinone compounds, several cell lines were also subjected to the same microscopic analysis [43]. As can be seen in Fig. 2A, when Q1 and Q23 were tested on several adherent cell lines (NIH3T3, L-cells, L-tk-, HeLa and HeLa-GFP), very similar toxicity effects were detected. Although the morphological changes of the dying cells resembled the changes attributed to apoptosis, it is clear that naphthoquinones can cause necrosis as well (see ref. [43] and references within). In order to determine if the two compounds, Q1 and Q23, induce similar modes of death, flow cytometry was utilized to help determine the percentages of cells undergoing necrosis and/or apoptosis. Annexin V-FITC staining, which detects phosphatidylserine exposure on the surface of apoptotic cells, and Propidium iodide (PI), which stains the nuclei of dying cells, were used in conjunction to determine the modes of death induced by Q1 and Q23.   As shown in Fig. 2B, treatment of a non-adherent lymphocyte cell line with Q1 and Q23 resulted in a significant induction of apoptosis ($\geq 30\%$; see [43]) consistent with prior results on the action of plumbagin and other naphthoquinones [46-49]. Although the cytotoxic effects of both quinones were quite similar, Q23 treatment resulted in a slightly higher level of necrosis (~30%) than apoptosis (~25%) at the highest concentrations tested (Fig. 2B). As will be discussed in the next section, it is likely that some of the naphthoquinone compounds that were recently screened will exhibit different modes of action.

1.6. USING THE HELA-GFP ASSAY TO DETERMINE THE CYTOTOXICITY OF ANTIBACTERIAL COMPOUNDS
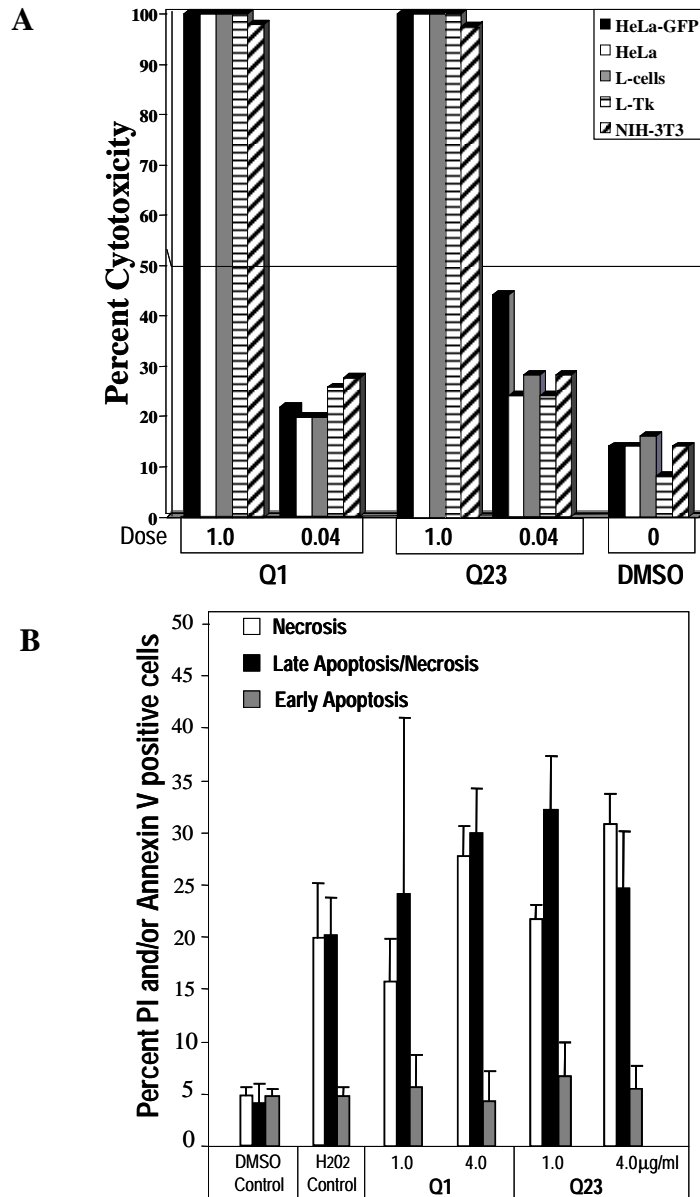
Figure 2. Analysis of the toxic effects of plumbagin (Q1) and Q23. (A) Cytotoxicity screening of Q1 and Q23 on various adherent cell lines. Plumbagin was tested at 5.3 (1.0) and 0.21 (.04) μM while Q23 was tested at 4.0 and 0.16 μM. DMSO (1 μl), which was the compound solvent, was added as a control at the same concentration as the test samples. (B) Graphical representation of results obtained by two-color flow cytometry (see [43]) at low and high compound concentration. Note that Annexin V-FITC and PI double staining should detect late apoptosis while single PI staining should be indicative of necrosis (see [43] for more details). Early apoptosis is defined as cells that are only Annexin V positive. Compounds were tested at the same concentration as in (A) for the lower concentration and four times that amount for the higher concentration.

Mycobacterial infections are on the increase worldwide, particularly in immunocompromised population, as is the case of *M. avium* in AIDS patients. Although these infections have devastating effects, there have been no new drugs specifically developed against these organisms since the 1960's ([50] and references within). A recent screen of acetophenone derivatives revealed that some of these compounds have significant anti-mycobacterial properties [50]. Acetophenone-derivaties with the strongest antibiotic properties were subsequently tested in the HeLa-GFP cytotoxicity assay to determine if any of these compounds exhibited cytotoxic effects against the human cell line (see Fig. 3; [50]). This analysis uncovered compounds with selective cytotoxicity toward eukaryotic cells (see asterisks, Fig. 3) and compounds with selective antibacterial activities (see arrows, Fig. 3; [50]). Thus, compounds likely to have distinct mechanisms of action in prokaryotic and eukaryotic organisms were uncovered. As will be described in more detail in the following section, a new 96-well assay has recently been developed that allows for the simultaneous screening of test compounds on gram positive and negative bacteria as well as on mammalian cells.
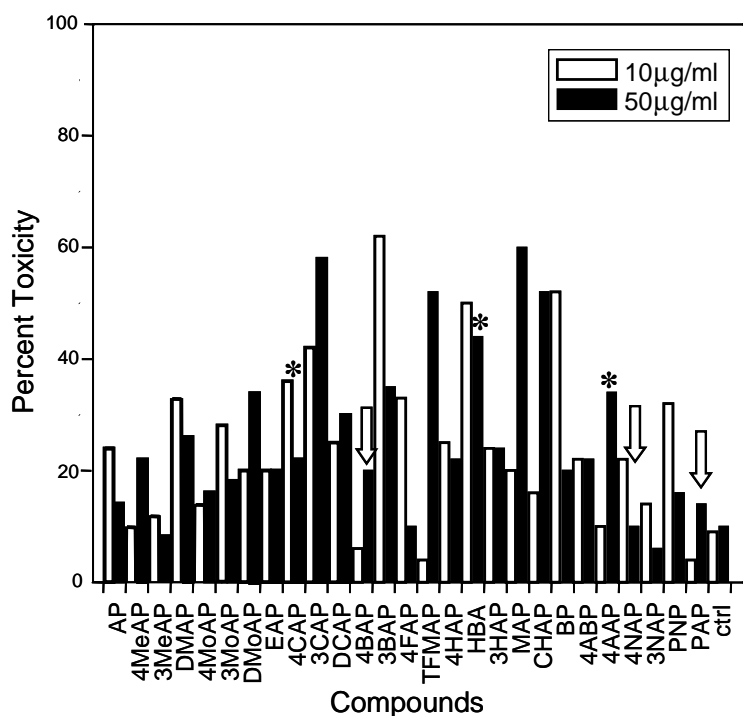
Figure 3. Screening of acetophenone compounds for toxicity with the HeLa-GFP assay. HeLa-GFP cells were exposed to various acetophenone compounds for 24 hours at two concentrations, 10 and 50 μg/ml. Compounds selectively toxic to bacteria (4 Nitroacetophenone, NAP; 4 Bromoacetophenone, 4BAP; and 4-Piperidinoacetophenone, PAP) with cytotoxicities of <25% and minimal inhibitory concentrations (MIC) of ≤ 605 are indicated with open arrows. Compounds selectively toxic to the HeLa cells (Hydroxybenzoic acid, HBA; 4-Chloroacetophenone, 4CAP; and 4-Aminoacetophenone, 4AAP) with cytotoxicity >25% and MIC >9500 are marked with asterisks (Ctrl, control without compound; see [50] for additional details).

1.7, LARGE-SCALE SCREENING OF COMPOUNDS ON EUKARYOTIC AND PROKARYOTIC CELLS

In order to rapidly screen novel compounds for their toxic properties, a relatively simple GFP-based assay was recently developed to simultaneously screen several compounds without having to perform other elaborate assays [43]. Although easy to implement, this assay could not be applied to high-throughput analysis as it relied on microscopic visualization [43]. Given this obvious limitation, the assay was modified to facilitate the simultaneous screening of multiple compounds in a 96-well format using an automated fluorescence plate reader. Since small quantities of compounds are analyzed, this assay is particularly well suited for the screening of small combinatorial chemical libraries. Another advantage of these microplate assays is the ability to perform all assays in duplicate or triplicate to derive more reliable results. Using this assay, we recently screened thirty nine naphthoquinone derivatives with significant success (see Fig.4 [44]).
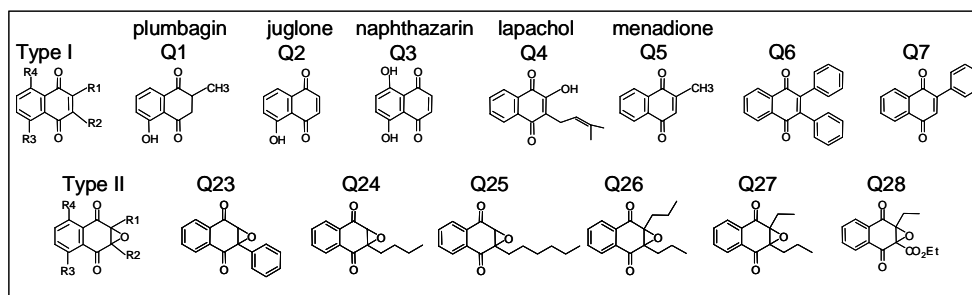
Figure 4. Chemical structure of some of the naphthoquinone compounds that were recently tested in the 96-well toxicity assays (see [44] for additional details). Type I compounds are prototypical naphthoquinones like plumbagin while Type II compounds represent naphthoquinone epoxides.

The HeLa-GFP assay was subsequently modified to test the same compounds on GFP-expressing *Escherichia coli* and *Mycobacterium avium* strains in an attempt to uncover potential anti-microbial agents [44]. As shown in Table 1, plumbagin (Q1) was clearly the most toxic of the test compounds on both the mammalian cells and the two bacterial strains. In addition, two similar compounds, Q3 (naphthazarin) and Q5 (menadione; Fig. 4) were also found to be highly toxic to all cell types. Apart from plumbagin, lapachol (Q4) was found to be the most toxic to *M. avium* as previously determined with other assays [51]. Interestingly, lapachol and similar quinones have recently been shown to exhibit strong inhibitory properties against two species of *Leishmania* associated to tegumentar leishmaniasis [52]. Although lapachol was found unsuitable as an anticancer drug due to its toxic side effects [53], it has recently been shown to exhibit anti-metastatic effects by inhibiting the invasiveness of cancer cells [54].

Most of the compounds tested exhibited the high levels of toxicity at higher concentrations, although some were still very toxic at a ten-fold dilution (see Q1-3 and Q23-25 at 2 µg/ml, Table 1) on the HeLa-GFP cell line. Apart from differences in

overall toxicity, two general types of toxic compounds were detected in these assays, those that exhibited toxicity to two or all three of the cell types (Q1-7 and Q23) and those that were primarily toxic to the HeLa cells (Q24-28; see Fig. 4). As these two sets of compounds apparently target different cell types, it is likely that these compounds will have different modes of action. Experiments are currently in progress to elucidate if these compounds have different molecular targets or if these differences are just a matter of membrane permeability. It is important to point out that the observed differences would not have been detected if the compounds had been tested on a single cell type.

Table 1. Percent GFP-fluorescence after chemical exposure

Compound	HeLa-GFP* 20 μg/ml**	HeLa-GFP 2 μg/ml	*E. coli*-GFP[+] 20 μg/ml	*M.avium*-GFP 20 μg/ml
Q1	9.0	13.0	1.0	7.0
Q2	29.0	14.0	111.0	72.0
Q3	4.0	0	41.0	38.0
Q4	3.0	70.0	56.0	26.0
Q5	22.0	13.0	58.0	69.0
Q6	20.0	78.0	105.0	55.0
Q7	25.0	13.0	89.0	35.0
Q23	3.0	14.0	56.0	66.0
Q24	23.0	5.0	87.0	202.0
Q25	18.0	0	118.0	133.0
Q26	27.0	26.0	110.0	97.0
Q27	21.0	21.0	117.0	133.0
Q28	4.0	17.0	115.0	97.0

* HeLa and *M. avium*-GFP cells were incubated with compound for 18 hrs.

**Compounds were tested at concentrations of 20 μg/ml or 2 μg/ml as indicated (see ref. [44]) .

[+]*E. coli*-GFP was incubated with compound for 10 hrs

A structural/physical analysis of the test compounds indicates that they exhibit significant differences in size, solubility (log P values) and toxicity (see Table 2 and [44] for additional details). For example, Type-1 compounds (see Fig. 4 and Table 1) generally exhibit high toxicity against all tested organisms, although *E. coli* was the most intrinsically resistant. In contrast, Type-2 compounds (see Table 1) were selectively toxic against the HeLa cells, perhaps due to some unique biotransformation in these cells. This analysis revealed that molecular weight and solubility (quantified as logP, see Table 2) of the compounds significantly correlated with toxicity to HeLa cells, with a weaker correlation of activity against *M. avium*, and did not correlate with killing of *E. coli* (for actual statistical values see [44]). Interestingly, toxicity against the two prokaryotic organisms strongly and significantly correlated with each other, but not with the eukaryotic cell line. This suggests that the mechanism of action of quinones is different against prokaryotic and eukaryotic cells, which has been observed in other studies as well [51]. In general, *M. avium* and *E. coli* were more tolerant to the

quinones than the HeLa cells. This is likely due to the great permeability barrier of mycobacteria [55] and the fact that *E. coli* often uses efflux pumps against quinones [56]. Compounds containing a 2,3-epoxide were highly toxic to eukaryotic cells (see Q23-Q28. Table 1), but were relatively non-toxic to prokaryotic cells. It thus appears that the differences between the mammalian and prokaryotic cells could be attributed to membrane permeability and/or cellular quinone metabolism.

Table 2. Names and physical characteristics of quinone compounds

Type-1* Compounds	Compound name	MW	LogP	R-group
Q1 Plumbagin	2-Methyl-5-hydroxy-1,4-naphtho quinone	188.18	0.87	$R_1=CH_3$; $R_2=H$ $R_3=OH$; $R_4=H$
Q2 Juglone	5-Hydroxy-1,4-naphthoquinone	174.15	1.92^+	$R_1=H$; $R_2=H$ $R_3=OH$; $R_4=H$
Q3 Naphthazarin	5,8-Dihydroxy-1,4-naphthoquinone	190.15	1.79^+	$R_1=H$; $R_2=H$ $R_3=OH$; $R_4=OH$
Q4 Lapachol	2-Hydroxy-3-(3-methylbut-2-enyl) - 1,4-naphthoquinone	242.27	2.02	$R_1=OH$ $R_2= CH_2CH=C(CH_3)_2$ $R_3=H$; $R_4=H$
Q5 Menadione	2-Methyl-1,4-naphthoquinone	172.18	2.20^+	$R_1=CH_3$; $R_2=H$ $R_3=H$; $R_4=H$
Q6	2,3-Diphenyl-1,4-naphthoquinone	310.35	3.99	$R_1=Ph$; $R_2=Ph$ $R_3=H$; $R_4=H$
Type-2 Compounds				
Q23	3-Phenyl-1,4-naphthoquinone oxide	250.25	1.74	$R_1=Ph$ $R_2=H$
Q24	3-Butyl-1,4-naphthoquinone oxide	230.26	1.67	$R_1=(CH_2)_3CH_3$ $R_2=H$
Q25	3-Hexyl-1,4-naphthoquinone oxide	258.31	2.50	$R_1=(CH_2)_5CH_3$ $R_2=H$
Q26	2,3-Propyl-1,4-naphthoquinone oxide	258.31	2.55	$R_1=CH_2CH_2CH_3$ $R_2= CH_2CH_2CH_3$
Q27	2-Ethyl-3-propyl-1,4naphthoquinone oxide	244.29	2.13	$R_1= CH_2CH_3$ $R2= CH_2CH_2CH_3$
Q28	2-Ethyl-3-(ethylperoxymethyl)-1,4-naphthoquinone oxide	274.27	1.42	$R_1=CH_2CH_3$ $R_2= CO_2CH_2CH_3$

 *Types1-2 naphthoquinones are based on structures shown in Fig. 4.
+ Experimental values for n-octanol-water, 25 °C.

1.8. SUMMARY:

The use of GFP as a biosensor has gained significant popularity over the last decade because this molecule can be utilized in a great variety of assays. Through the use of cell-based assays, this fluorescent marker has facilitated the *in vivo* and *in situ* visualization of proteins that are involved in complex cellular functions. Although several GFP-based models have already been applied to the screening of toxic, anticancer, and antibacterial compounds, it is clear that improvements in these assays

will greatly advance the field of drug discovery. As described in this review, we have developed simple and effective assays to determine the toxicity of various compounds on various cell types. Furthermore, these assays can be performed in parallel to screen for toxic compounds on both eukaryotic and prokaryotic cells in a cost effective and reproducible manner. The availability of sophisticated instrumentation and robotic systems should soon allow for the implementation of the aforementioned assays to high-throughput screening of thousands of compounds from established and/or new chemical libraries.

1.9. ACKNOWLEDGEMENTS:

2.0. REFERENCES

1. O.Shimomura, The discovery of aequorin and green fluorescent protein, J.Microsc. 217, (2005) 1-15.
2. D.C.Prasher, V.K.Eckenrode, W.W.Ward, F.G.Prendergast, M.J.Cormier, Primary structure of the Aequorea victoria green-fluorescent protein, Gene 111, (1992) 229-233.
3. J.Lippincott-Schwartz, G.H.Patterson, Development and use of fluorescent protein markers in living cells, Science 300, (2003) 87-91.
4. D.C.Prasher, Using GFP to see the light, Trends Genet. 11, (1995) 320-323.
5. J.C.March, G.Rao, W.E.Bentley, Biotechnological applications of green fluorescent protein, Appl.Microbiol.Biotechnol. 62, (2003) 303-315.
6. A.W.Knight, Using yeast to shed light on DNA damaging toxins and irradiation, Analyst 129, (2004) 866-869.
7. O.Griesbeck, Fluorescent proteins as sensors for cellular functions, Curr.Opin. Neurobiol. 14, (2004) 636-641.
8. S.J.Rosochacki, M.Matejczyk, Green fluorescent protein as a molecular marker in microbiology, Acta Microbiol.Pol. 51, (2002) 205-216.
9. A.W.Knight, P.O.Keenan, N.J.Goddard, P.R.Fielden, R.M.Walmsley, A yeast-based cytotoxicity and genotoxicity assay for environmental monitoring using novel portable instrumentation, J.Environ.Monit. 6, (2004) 71-79.
10. A.W.Knight, N.J.Goddard, N.Billinton, P.A.Cahill, R.M.Walmsley, Fluorescence polarization discriminates green fluorescent protein from interfering autofluorescence in a microplate assay for genotoxicity, J.Biochem.Biophys. Methods 51, (2002) 165-177.

11. P.A.Cahill, A.W.Knight, N.Billinton, M.G.Barker, L.Walsh, P.O.Keenan, C.V. Williams, D.J.Tweats, R.M.Walmsley, The GreenScreen genotoxicity assay: a screening validation programme, Mutagenesis 19, (2004) 105-119.

12. A.Norman, H.L.Hestbjerg, S.J.Sorensen, Construction of a ColD cda promoter-based SOS-green fluorescent protein whole-cell biosensor with higher sensitivity toward genotoxic compounds than constructs based on recA, umuDC, or sulA promoters, Appl.Environ.Microbiol. 71, (2005) 2338-2346.

13. K.E.Sandman, S.S.Marla, G.Zlokarnik, S.J.Lippard, Rapid fluorescence-based reporter-gene assays to evaluate the cytotoxicity and antitumor drug potential of platinum complexes, Chem.Biol. 6, (1999) 541-551.

14. A.M.Steff, M.Fortin, C.Arguin, P.Hugo, Detection of a decrease in green fluorescent protein fluorescence for the monitoring of cell death: an assay amenable to high-throughput screening technologies, Cytometry 45, (2001) 237-243.

15. M.Beckman, M.Kihlmark, K.Iverfeldt, E.Hallberg, Degradation of GFP-labelled POM121, a non-invasive sensor of nuclear apoptosis, precedes clustering of nuclear pores and externalisation of phosphatidylserine, Apoptosis. 9, (2004) 363-368.

16. N.V.Gorbunov, J.E.Morris, J.S.Greenberger, B.D.Thrall, Establishment of a novel clonal murine bone marrow stromal cell line for assessment of p53 responses to genotoxic stress, Toxicology 179, (2002) 257-266.

17. A.Quinones, N.G.Rainov, Identification of genotoxic stress in human cells by fluorescent monitoring of p53 expression, Mutat.Res. 494, (2001) 73-85.

18. N.Kienzle, S.Olver, K.Buttigieg, A.Kelso, The fluorolysis assay, a highly sensitive method for measuring the cytolytic activity of T cells at very low numbers, J.Immunol.Methods 267, (2002) 99-108.

19. H.Harada, K.Saijo, I.Ishiwata, T.Ohno, A GFP-transfected HFWT cell line, GHINK-1, as a novel target for non-RI activated natural killer cytotoxicity assay, Hum.Cell 17, (2004) 43-48.

20. V.Bobek, J.Plachy, D.Pinterova, K.Kolostova, M.Boubelik, P.Jiang, M.Yang, R.M.Hoffman, Development of a green fluorescent protein metastatic-cancer chick-embryo drug-screen model, Clin.Exp.Metastasis 21, (2004) 347-352.

21. P.H.Krone, S.R.Blechinger, T.G.Evans, J.A.Ryan, E.J.Noonan, L.E.Hightower, Use of fish liver PLHC-1 cells and zebrafish embryos in cytotoxicity assays, Methods 35, (2005) 176-187.

22. S.R.Blechinger, J.T.Warren, Jr., J.Y.Kuwada, P.H.Krone, Developmental toxicology of cadmium in living embryos of a stable transgenic zebrafish line, Environ.Health Perspect. 110, (2002) 1041-1046.

23. K.Kurauchi, Y.Nakaguchi, M.Tsutsumi, H.Hori, R.Kurihara, S.Hashimoto, R.Ohnuma, Y.Yamamoto, S.Matsuoka, S.Kawai, T.Hirata, M.Kinoshita, In vivo visual reporter system for detection of estrogen-like substances by transgenic medaka, Environ.Sci.Technol. 39, (2005) 2762-2768.

24. A.L.Graves, W.A.Boyd, P.L.Williams, Using transgenic Caenorhabditis elegans in soil toxicity testing, Arch.Environ.Contam Toxicol. 48, (2005) 490-494.

25. M.Yang, L.Li, P.Jiang, A.R.Moossa, S.Penman, R.M.Hoffman, Dual-color fluorescence imaging distinguishes tumor cells from induced host angiogenic vessels and stromal cells, Proc.Natl.Acad.Sci.U.S.A 100, (2003) 14259-14262.

26. M.Yang, E.Baranov, J.W.Wang, P.Jiang, X.Wang, F.X.Sun, M.Bouvet, A.R.Moossa, S.Penman, R.M.Hoffman, Direct external imaging of nascent cancer, tumor progression, angiogenesis, and metastasis on internal organs in the fluorescent orthotopic model, Proc.Natl.Acad.Sci.U.S.A 99, (2002) 3824-3829.

27. S.Paris, R.Sesboue, Metastasis models: the green fluorescent revolution? Carcinogenesis 25, (2004) 2285-2292.

28. R.M.Hoffman, Imaging tumor angiogenesis with fluorescent proteins, APMIS 112, (2004) 441-449.

29. X.Xie, Z.Luo, K.M.Slawin, D.M.Spencer, The EZC-prostate model: noninvasive prostate imaging in living mice, Mol.Endocrinol. 18, (2004) 722-732.

30. K.Yamauchi, M.Yang, P.Jiang, N.Yamamoto, M.Xu, Y.Amoh, K.Tsuji, M.Bouvet, H.Tsuchiya, K.Tomita, A.R.Moossa, R.M.Hoffman, Real-time in vivo dual-color imaging of intracapillary cancer cell and nucleus deformation and migration, Cancer Res. 65, (2005) 4246-4252.

31. R.M.Hoffman, In vivo imaging with fluorescent proteins: the new cell biology, Acta Histochem. 106, (2004) 77-87.

32. G.Choy, P.Choyke, S.K.Libutti, Current advances in molecular imaging: noninvasive in vivo bioluminescent and fluorescent optical imaging in cancer research, Mol.Imaging 2, (2003) 303-312.

33. T.Umeoka, T.Kawashima, S.Kagawa, F.Teraishi, M.Taki, M.Nishizaki, S.Kyo, K.Nagai, Y.Urata, N.Tanaka, T.Fujiwara, Visualization of intrathoracically disseminated solid tumors in mice with optical imaging by telomerase-specific amplification of a transferred green fluorescent protein gene, Cancer Res. 64, (2004) 6259-6265.

34. J.Condeelis, R.Singer, J.E.Segall, The Great Escape: When cancer cells hijack the genes for chemotaxis and motility, Annu.Rev.Cell Dev.Biol. (2005).

35. E.Sahai, J.Wyckoff, U.Philippar, J.E.Segall, F.Gertler, J.Condeelis, Simultaneous imaging of GFP, CFP and collagen in tumors in vivo using multiphoton microscopy, BMC.Biotechnol. 5, (2005) 14.

36. D.B.Kassel, Applications of high-throughput ADME in drug discovery, Curr.Opin.Chem.Biol. 8, (2004) 339-345.

37. J.R.Kenseth, S.J.Coldiron, High-throughput characterization and quality control of small-molecule combinatorial libraries,Curr.Opin.Chem.Biol. 8, (2004) 418-423.

38. L.Zemanova, A.Schenk, M.J.Valler, G.U.Nienhaus, R.Heilker, Confocal optics microscopy for biochemical and cellular high-throughput screening, Drug Discov.Today 8, (2003) 1085-1093.

39. W.H.van de, E.Gifford, ADMET in silico modelling: towards prediction paradise? Nat.Rev.Drug Discov. 2, (2003) 192-204.

40. M.T.Cronin, Prediction of drug toxicity Farmaco 56, (2001) 149-151.

41. K.S.Lam, Application of combinatorial library methods in cancer research and drug discovery, Anticancer Drug Des 12, (1997) 145-167.

42. M.D.Burke, S.L.Schreiber, A planning strategy for diversity-oriented synthesis, Angew.Chem.Int.Ed Engl. 43, (2004) 46-58.

43. J.Montoya, A.Varela-Ramirez, A.Estrada, L.E.Martinez, K.Garza, R.J.Aguilera, A fluorescence-based rapid screening assay for cytotoxic compounds, Biochem.Biophys.Res.Commun. 325, (2004) 1517-1523.

44. J.Montoya, A.Varela-Ramirez, M.Shanmugasundram, L.E.Martinez, T.P.Primm, R.J.Aguilera, Tandem screening of toxic compounds on GFP-labeled bacteria and cancer cells in microtiter plates, Biochem.Biophys.Res.Commun. (2005; in press).
45. T.Kanda, K.F.Sullivan, G.M.Wahl, Histone-GFP fusion protein enables sensitive analysis of chromosome dynamics in living mammalian cells, Curr.Biol. 8, (1998) 377-385.
46. J.J.Inbaraj, C.F.Chignell, Cytotoxic action of juglone and plumbagin: a mechanistic study using HaCaT keratinocytes, Chem.Res.Toxicol. 17, (2004) 55-62.
47. D.W.Lamson, S.M.Plaza, The anticancer effects of vitamin K, Altern.Med.Rev. 8, (2003) 303-318.
48. M.Krishnaswamy, K.K.Purushothaman, Plumbagin: A study of its anticancer, antibacterial & antifungal properties, Indian J.Exp.Biol. 18, (1980) 876-877.
49. M.Kaminski, M.Karbowski, Y.Miyazaki, J.Kedzior, J.H.Spodnik, A.Gil, M.Wozniak, T.Wakabayashi, Co-existence of apoptotic and necrotic features within one single cell as a result of menadione treatment, Folia Morphol.(Warsz.) 61, (2002) 217-220.
50. L.Rajabi, C.Courreges, J.Montoya, R.J.Aguilera, T.P.Primm, Acetophenones with selective antimycobacterial activity, Lett.Appl.Microbiol. 40, (2005) 212-217.
51. T.Tran, E.Saheba, A.V.Arcerio, V.Chavez, Q.Y.Li, L.E.Martinez, T.P.Primm, Quinones as antimycobacterial agents, Bioorg.Med.Chem. 12, (2004) 4809-4813.
52. N.M.Lima, C.S.Correia, L.L.Leon, G.M.Machado, M.F.Madeira, A.E.Santana, M.O.Goulart, Antileishmanial activity of lapachol analogues, Mem.Inst.Oswaldo Cruz 99, (2004) 757-761.
53. J.B.Block, A.A.Serpick, W.Miller, P.H.Wiernik, Early clinical studies with lapachol (NSC-11905), Cancer Chemother.Rep.2 4, (1974) 27-28.
54. I.T.Balassiano, S.A.De Paulo, S.N.Henriques, M.C.Cabral, M. da Gloria da Costa Carvalho, Demonstration of the lapachol as a potential drug for reducing cancer metastasis, Oncol.Rep. 13, (2005) 329-333.
55. H.Nikaido, Preventing drug access to targets: cell surface permeability barriers and active efflux in bacteria, Semin.Cell Dev.Biol. 12, (2001) 215-223.
56. G.Tegos, F.R.Stermitz, O.Lomovskaya, K.Lewis, Multidrug pump inhibitors uncover remarkable activity of plant antimicrobials, Antimicrob.Agents Chemother. 46, (2002) 3133-3141.